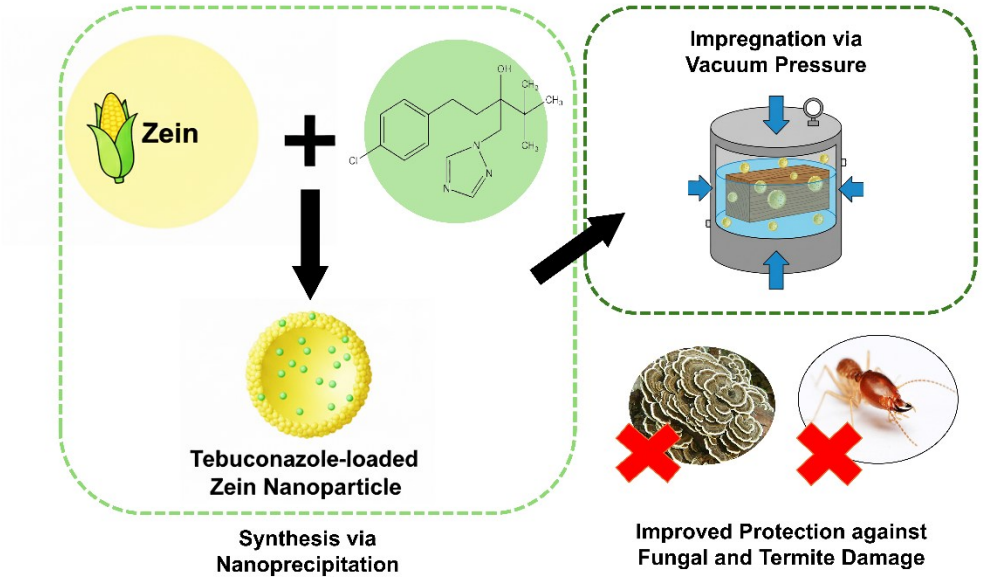
Sustained-Release Tebuconazole-Loaded Zein Nanoparticles for Enhanced Rubberwood Preservation *via* Nanoprecipitation

Zhexun Ong,[a] Mohamad Nasir Mat Arip ,[b] Shahlinney Lipeh ,[c] Arnaud Besserer ,[d] Nicolas Brosse ,[d] G. Veera Singham ,[e] and Hooi Ling Lee [a,*]

*Corresponding author: hllee@usm.my

DOI: 10.15376/biores.21.3.7801-7822

GRAPHICAL ABSTRACT



Sustained-Release Tebuconazole-Loaded Zein Nanoparticles for Enhanced Rubberwood Preservation *via* Nanoprecipitation

Zhexun Ong,[a] Mohamad Nasir Mat Arip ,[b] Shahlinney Lipeh ,[c] Arnaud Besserer ,[d] Nicolas Brosse ,[d] G. Veera Singham ,[e] and Hooi Ling Lee [a,*]

Rubberwood (*Hevea brasiliensis*), a widely utilised timber in Malaysia, is susceptible to degradation from fungi and termites, requiring effective preservation strategies to extend its service life. This study explores a novel approach for improving the delivery of tebuconazole (TEB), a triazole fungicide, into rubberwood using zein nanoparticles prepared *via* the nanoprecipitation method. The optimised zein nanoparticles achieved a hydrodynamic size of 146.4 ± 10.66 nm with a loading efficiency of 43.0%. The treated rubberwood samples were categorised as "easily treated" and showed sustained release of TEB from leaching tests. Results showed good protection against subterranean termites (*Coptotermes gestroi*) with promising resistance to brown rot (*Gloeophyllum trabeum*) and white rot (*Trametes versicolor*) fungi. The study highlights the potential of nanoprecipitation as a sustainable, efficient alternative to traditional wood preservation methods, offering reduced chemical usage and improved delivery efficiency.

DOI: 10.15376/biores.21.3.7801-7822

Keywords: Wood preservation; Nanoparticles; Nanotechnology; Nanoprecipitation; Zein; Tebuconazole; Infrared spectroscopy; Leaching test; Preservative delivery

*Contact information: a: Nanomaterials Research Group, School of Chemical Sciences, Universiti Sains Malaysia, 11800 USM, Penang, Malaysia; b: Technical Services Division, Forest Research Institute Malaysia (FRIM), 52109 Kepong, Selangor Darul Ehsan, Malaysia; c: Forest Products Division, Forest Research Institute Malaysia, 52109 Kepong, Selangor, Malaysia; d: Université de Lorraine, INRAE, LERBMAB, GP4W, F 54000 Nancy, France; e: Centre for Chemical Biology, Universiti Sains Malaysia, 10 Persiaran Bukit Jambul, 11900 Penang, Malaysia; *Corresponding author: hllee@usm.my*

INTRODUCTION

Wood is an essential, renewable resource widely used across various industries, including construction, furniture manufacturing, and musical instruments (Chen *et al.* 2020). Its versatile properties, such as strength-to-weight ratio, durability, and thermal insulation, attract many applications (Ramage *et al.* 2017; Jakob *et al.* 2022). Rubberwood (*Hevea brasiliensis*), a byproduct of the rubber industry, has become an important source of timber, especially in Southeast Asia. Rubberwood is primarily used in furniture, flooring, and other wood-based products due to its relatively low cost and good mechanical properties. Malaysia, a significant rubberwood producer, has relied heavily on rubberwood for the furniture industry, contributing substantially to its economic output (Shigematsu *et al.* 2011; Teoh *et al.* 2011). The *sape*, a traditional Sarawakian instrument, is often made with rubberwood, which holds significance to Malaysian culture (Wong *et al.* 2023).

However, despite its advantages, rubberwood faces several challenges that can limit its use and durability.

One of the most significant issues with rubberwood is its susceptibility to degradation, primarily caused by biotic and abiotic factors. Rubberwood, like many other wood types, is prone to attacks from white rot and brown rot fungi; in addition, it is susceptible to termites like subterranean termites, which are common in Southeast Asia (Nazarpour *et al.* 2013; Teoh *et al.* 2011). These biotic factors are responsible for wood degradation, which can lead to a considerable loss of material strength and aesthetics. Untreated or unmodified rubberwood is highly susceptible to fungal and termite attacks, which compromise its lifespan, durability, and usability (Nazarpour *et al.* 2013). The aesthetic and acoustic properties of wood are integrated in many regional cultures, making the degradation of timber a threat not only to structural integrity, but also to tools and musical instruments and to the continuity of these heritage practices and values.

To address these concerns, wood preservation techniques have been developed to extend the service life of wood by preventing or slowing down the process of degradation. Wood preservatives are chemical substances that are applied to wood to protect it from the damaging effects of biotic and abiotic factors. Commonly used preservatives include oil-borne, water-borne, and chemical-based formulations that are designed to be either absorbed into the wood matrix or applied to its surface (Hassan *et al.* 2021; Vani *et al.* 2022). The application of these preservatives is essential for maintaining the structural integrity and functionality of wood, particularly in outdoor or high-moisture environments where degradation is more likely to occur (Cheremisinoff and Rosenfeld 2010; Alade *et al.* 2022).

However, the widespread use of traditional wood preservatives presents several environmental and health-related issues. Many of the chemical preservatives in use today contain toxic substances, such as heavy metals and biocides, which can leach into the environment, contaminating soil, water, and surrounding ecosystems (Chaud *et al.* 2021; Khademibami and Bobadilha 2022; Emenike *et al.* 2024). For example, preservatives such as chromated copper arsenate (CCA), ammoniacal copper zinc arsenate (ACZA), and pentachlorophenol contain toxic compounds such as chromium, arsenic, and chlorine, which are harmful to both human health and wildlife (Ohgami *et al.* 2015; Kato *et al.* 2021; Emenike *et al.* 2024). The leaching of these toxic chemicals from treated wood into the environment is a major concern, particularly in areas where the treated wood is exposed to rain or moisture (Townsend *et al.* 2004; Thaler and Humar 2014).

Considering these environmental and health concerns, there has been increasing interest in the development of safer and more sustainable wood preservation methods. One alternative is the use of organic biocides, which are biodegradable and less harmful to the environment compared to traditional chemical preservatives (Lebow 2010). Among these biocides, tebuconazole (TEB), a triazole-based fungicide, can protect wood against brown rot (*Gloeophyllum trabeum*) and white rot fungi (*Trametes versicolor*) (de Albuquerque *et al.* 2018; Tleuova *et al.* 2020). TEB functions by inhibiting the biosynthesis of ergosterol, a critical component of fungal cell membranes, thereby disrupting fungal growth and preventing wood decay (de Albuquerque *et al.* 2018). Its effectiveness against wood-damaging fungi has made it a viable candidate for use in wood preservation.

Despite its promising antifungal properties, TEB has limitations that hinder its practical application, primarily its challenge associated with poor solubility in water, which limits its ability to be effectively incorporated into wood preservation systems that rely on water as the medium for delivery (Čadková *et al.* 2013). This issue increases the difficulty

of applying TEB using conventional pressure treatment methods, such as the full-cell or modified full-cell vacuum pressure techniques, which require TEB to be delivered through an aqueous medium, necessitating higher concentrations for adequate protection, and resulting in insoluble TEB in the water medium, causing health and environmental hazards to soil and earthworms (Chen *et al.* 2018).

To overcome this limitation, alternative delivery systems have been explored, such as the use of nanoparticles to encapsulate hydrophobic substances on TEB (Díaz-Blancas *et al.* 2016; Ong *et al.* 2023). Nanotechnology has emerged as a promising tool for improving the solubility, stability, and controlled release of poorly soluble compounds. Among the various nanomaterials available, zein nanoparticles (zein NPs) have gained significant attention for their ability to encapsulate hydrophobic drugs and active ingredients. Zein is a natural, biodegradable protein derived from corn, which allows it to interact with both hydrophobic and hydrophilic substances with its amphiphilic properties (da Rosa *et al.* 2015; Araujo *et al.* 2021; Campos *et al.* 2023). This makes zein an ideal candidate for use as a carrier, particularly for the hydrophobic TEB.

Zein NPs are typically prepared using methods such as nanoprecipitation, where a solvent containing the zein and active ingredient is introduced into an aqueous phase, leading to the formation of nanoparticles (Hu and McClements 2014; Li *et al.* 2019; Xing *et al.* 2022). These nanoparticles can encapsulate TEB, improving its solubility and stability in water, thus enhancing its delivery into the wood matrix. Additionally, the use of zein as a carrier material offers the benefit of biocompatibility and biodegradability, ensuring that the preservation treatment is environmentally friendly and sustainable (Xing *et al.* 2022; Campos *et al.* 2023). By using zein NPs to deliver TEB, the limitations associated with TEB's poor solubility can be mitigated, allowing for more effective wood preservation treatments.

The potential application of zein NPs in wood preservation was explored in this study, where TEB-loaded zein NPs were synthesised using the nanoprecipitation method and characterized using dynamic light scattering (DLS), FTIR, SEM-EDX, UV-Vis spectroscopy, TGA, and DSC. The optimised NPs were applied to rubberwood through a modified full-cell vacuum pressure treatment. The treated wood was tested against subterranean termites, brown rot and white rot fungi to observe the effectiveness of the preservative delivery approach.

EXPERIMENTAL

Materials

For the synthesis of zein NPs, pure zein powder (88% protein, Thermo Fischer, USA), Tween 80 (polysorbate 80, Fischer Scientific, United Kingdom), and 99.5% ethanol (Grade AR, QReC, Malaysia) were purchased from respective suppliers. Tebuconazole (97%, Sigma Aldrich, USA), rubberwood (*Hevea brasiliensis*) specimens, brown rot (*Gloeophyllum trabeum*), and white rot (*Trametes versicolor*) fungi cultures were provided by Forest Research Institute Malaysia, whereas subterranean termites (*Coptotermes gestroi*) were provided by the Centre of Chemical Biology, USM.

Formulation Development of TEB-loaded Zein NPs

The fabrication of blank zein NPs references the pH antisolvent method with minor modifications (Hu and McClements 2014). First, 0.02%w/v zein was prepared in 85%

ethanol as the solvent phase, while 0.02%v/v polysorbate 80 was prepared in distilled water as the aqueous phase. Next, 5 mL of the solvent phase was added dropwise to the aqueous phase using a controlled syringe pump setup with dropping rate of 0.2 mL/min, and the solution was stirred at 1000 rpm using a magnetic stirrer. The solution was stirred for another 2 h at constant room temperature and airflow to remove ethanol through evaporation. The solution was then processed stepwise (Table 1) to remove possible impurities and to obtain the finalized NPs.

Table 1. Processing of TEB-loaded Zein Nanoparticles

Process step	Parameters
Centrifugation	4000 rpm for 10 min
Washing	Two times with distilled water
Freeze-drying	12 hours

Subsequently, parameters such as zein concentration, polysorbate 80 concentration, dropping rate, pH, zein: TEB ratio, and solvent: aqueous phase ratio were systematically varied using a one-variable-at-a-time approach to optimise the NPs to minimise particle size and maximise the loading efficiency of TEB in the zein NPs. To measure TEB loading efficiency in TEB-loaded zein NPs, 10 mg of nanoparticles and blank zein NPs were weighed accurately and transferred to respective 10 mL Falcon tubes, followed by mixing with 3 mL of 50% aqueous ethanol. Both samples were sonicated for 10 min to extract TEB. The samples were centrifuged at 4,000 rpm for 5 min. The supernatant from both samples was scanned using a UV-Vis spectrometer to determine their λ_{max}, absorbance value, and subsequently, their respective concentrations. Each measurement was done in triplicate, and the average value was calculated with Eq. 1.

$$\text{Loading efficiency} = \frac{(\text{TEB loaded concentration} - \text{TEB blank concentration})}{\text{TEB loaded concentration}} \quad (1)$$

Methods

Spectrum analysis of the samples was done using ATR-FTIR spectrometer (PerkinElmer Spotlight 200, USA), with all samples recorded from 600 to 4000 cm^{-1} at a resolution of 4 cm^{-1} and 16 scans. The NPs were analysed with dynamic light scattering (DLS) (Malvern Zetasizer Nano ZS, UK) to determine the hydrodynamic size of the NPs, with the measurements taken 25 °C, and the viscosity and refractive index of water were set at 0.89 cP and 1.33, respectively. Approximately 10 mg of NPs were weighed and dispersed in 10 mL of distilled water, followed by 5 min of sonication. The samples were filtered through a 0.45 µm pore size polyvinylidene fluoride syringe filter into the plastic cuvette cell for analysis. To determine the morphology and composition of the zein NPs, scanning electron microscopy-energy dispersive X-ray (SEM-EDX) (Hitachi-Regulus, Japan) was used to analyse the NPs at 1.0 kV. Loading efficiency of TEB in the zein NPs was performed using UV-visible spectroscopy (Shimadzu UV-2700i, Japan). An accurate mass of 10 mg of both the TEB-loaded zein NPs and blank zein NPs was weighed and transferred into separate 10 mL Falcon tubes. Each sample was then mixed with 3 mL of 50% aqueous ethanol and subjected to sonication for 10 min to extract the loaded TEB. The samples were centrifuged at 4,000 rpm for 5 min. The supernatant from each sample was collected and analysed to determine the λ_{max}, absorbance, and corresponding concentrations of TEB. All measurements were performed in triplicate, and the mean value

was subsequently calculated. Thermogravimetric analysis (TGA) (PerkinElmer STA 6000, USA) and differential scanning calorimetry (DSC) (PerkinElmer Pyris 1, USA), respectively, were used to assess the thermal stability and phase transitions of the NPs. TGA was performed with a heating rate of 10 °C/min from 0 to 800 °C under a nitrogen atmosphere, whereas DSC was conducted at 10 °C/min from 0 to 250 °C under a nitrogen atmosphere.

Validation of UV-Visible spectrophotometric method for determination of tebuconazole (TEB) in TEB-loaded zein NP

The quantification of TEB loaded within the NPs was performed using UV-Visible spectrophotometry. The method's accuracy, precision, and reproducibility for determining TEB presence and concentration were validated. For these validation studies, a 50 ppm ethanolic TEB stock solution was prepared and subsequently diluted to generate a series of standards ranging from 5 ppm to 30 ppm. The absorbance of these standards was then measured, using 85% ethanol as the blank, to construct a calibration curve plotting TEB concentrations (x-axis) against their corresponding absorbance values (y-axis). In the Appendix, Fig. A1 and Table A1, A2, and A3 provide the statistical analysis of the validation.

Rubberwood treatment of TEB-loaded zein NPs

Rubberwood (*Hevea brasiliensis*) were treated with TEB-loaded zein NPs with a modified full cell vacuum pressure treated according to the Malaysian Standard (MS360:1991). Rubberwood samples were measured to 25 × 25 × 6 mm and were initially air-dried until they achieved a constant weight ($W_{initial}$). The samples were then placed in a desiccator and subjected to a vacuum of no less than -80 kPa for a minimum duration of 60 min to facilitate the removal of any impurities within the wood's pore structure. Subsequently, the samples were immersed in the solution with TEB-loaded zein NPs and were pressure-treated with 340 kPa for 60 min. Once the pressure was released, the samples were removed from the desiccator, allowed to air-dry for 30 min, and reweighed (denoted as W_{AD}). The samples were then subjected to an oven-drying process at 100 °C for 12 h, until a constant weight (W_{OD}) was achieved. Using the recorded weights, the treatability and chemical retention of TEB-loaded zein NPs in the wood samples were determined. Control samples were treated with distilled water under the same experimental conditions. Treatability refers to "the measure of extent to which a porous material can be impregnated with liquids" (Tarmian *et al.* 2020), whereas chemical retention is defined as "the amount of wood preservative that remains in the wood sample after treatment" (Islam *et al.* 2014). Treatability and chemical retention are calculated using Eq. 2 and 3, where G is the is the specific gravity of TEB at 1.249 g/cm^3, and V is the volume of the wood sample.

$$\text{Treatability } (l\text{m}^{-3}) = \frac{W_{AD}\text{-}W_{OD}}{G*V} \times 1000 \quad (2)$$

$$\text{Chemical retention } (\text{kgm}^{-3}) = \text{Treatability} \times \frac{\text{concentration of solution (\%w/w)}}{100} \quad (3)$$

Leaching studies were conducted to evaluate the efficacy of the delivery approaches into the wood and their potential to withstand real-world weathering conditions. The leaching test procedure was modified according to EN 84. Wood samples were immersed in deionised water at a 1:5 (wood volume : water volume) ratio. The water was replenished

after 24 and 48 h, with a total of seven water changes performed over the initial 12-day period, extending the total immersion to 14 days. Subsequently, water changes were conducted every two days for an additional 30 days. The resulting leachates were collected and stored in Falcon tubes at a consistent room temperature for subsequent quantification of TEB content *via* UV-Vis spectrophotometry. Permeability ratings are given in Table A4, whereas wood durability ratings for anti-termite tests and weight loss classification for anti-fungi tests were defined in Table A5 and A6 respectively.

Biological efficacy testing for TEB-loaded zein NP treated wood

The rubberwood treated with TEB-loaded zein NPs is tested against brown rot (*Gloeophyllum trabeum*), white rot fungi (*Trametes versicolor*), and subterranean termite (*Coptotermes gestroi*). The anti-fungi study followed ASTM D2017-05 (2005), whereas the anti-termite study followed the ASTM D3345-08 (2017). Weight loss was calculated using wood samples before and after the tests, and their decay rating was evaluated. Triplicates were prepared for each parameter.

RESULTS AND DISCUSSION

The FTIR analysis was used to confirm the presence of TEB and zein through the examination of functional groups, and possible interactions from the incorporation of TEB into the zein matrix to identify any potential chemical interactions that may influence the properties and performance of the NPs. The FTIR spectra of the blank zein NP, TEB-loaded zein NP, and pure TEB were compared to investigate the characteristic bands of each component in Fig. 1. The spectrum of blank zein NPs displayed characteristic bands of the protein. The broad peak observed at 3287 cm^{-1} corresponds to the O-H stretching vibration of amide groups, while the bands at 1642 cm^{-1} and 1530 cm^{-1} are attributed to the C=O stretching and N-H bending vibrations, respectively, within the protein backbone (Hu *et al.* 2015; Zou *et al.* 2012). For the TEB-loaded zein NPs, additional bands related to TEB were observed, including a prominent peak at 1449 cm^{-1} representing N-N stretching, and aromatic C-C stretching at 1534 cm^{-1}. Weak C-Cl stretching was observed at 700 cm^{-1} in the loaded zein NP spectrum, but it was absent in the blank zein NP, which confirms the presence of TEB in the loaded zein NPs (De Lorenzi *et al.* 1999). There were no significant peak shifts of C-Cl; hence, it is suggested that TEB is adsorbed onto the zein NPs.

Multiple optimisation parameters were identified to influence NP size through DLS analysis, with the trends displayed in Fig. 2a to f, with further details listed in Tables A7 to A12. Lower zein concentrations promoted instability and aggregation, while higher concentrations led to saturation and size increase (Hu and McClements 2015; Patel *et al.* 2010). Polysorbate 80 at 0.035% w/v provided steric stabilisation, yielding the smallest particles. The effect of increasing polysorbate 80 concentration diminishes, as the presence of the surfactant is effective enough to stabilise the formation of the zein NP (Hu and McClements 2014; Sivasankar *et al.* 2024). The dropping rate of 0.6 mL/min enabled effective mixing without inducing oversaturation, as faster rates introduced the solvent phase too quickly and saturate the mixture with high zein concentration, leading to fewer but larger particles due to nucleation kinetics (Saad and Prud'homme 2016).

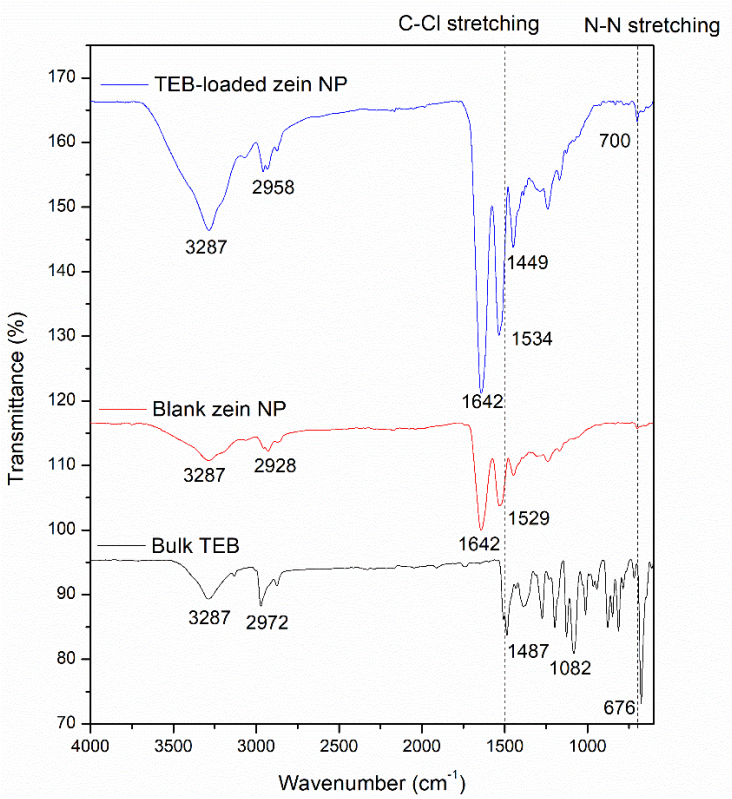


Fig. 1. FTIR spectra of TEB-loaded zein NP, blank zein NP, and bulk TEB

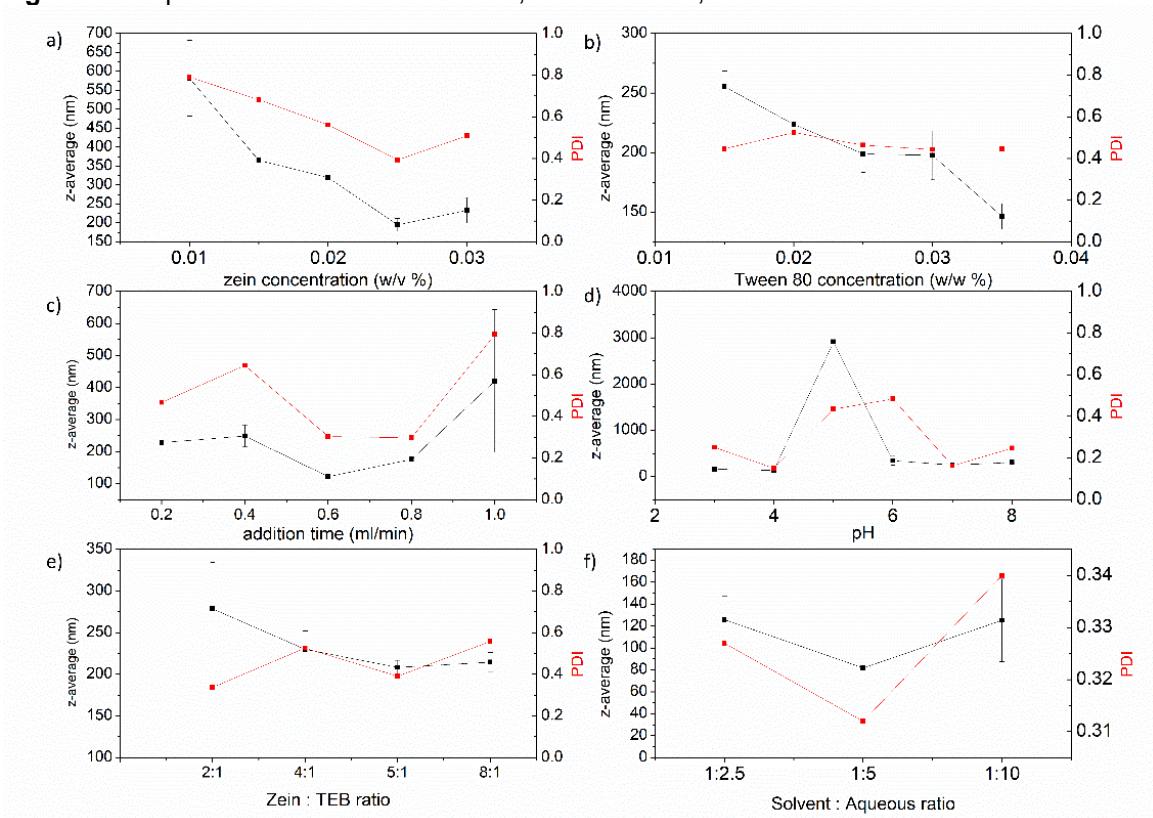


Fig. 2. Various parameter effects on nanoparticle size and PDI of a) zein concentration, b) polysorbate 80 concentration, c) addition time, d) pH, e) zein: TEB ratio, and f) solvent: aqueous ratio

Zein is heavily influenced by pH due to its protein nature, and its isoelectric point is near 6.2 (Podaralla and Perumal 2010). Thus, adjusting the pH in the process will modify the NP size. The pH adjustment in the aqueous phase provided low ionic strength and prevented aggregation from the nanoprecipitation, which was similar to previous studies (Sivasankar *et al.* 2024). At pH 4, strong electrostatic repulsion among positively charged zein molecules prevented aggregation. As pH increases, deprotonation causes zein side chains to repel each other and encourage smaller particles, albeit yielding larger hydrodynamic sizes than at lower pH (Wang *et al.* 2024a). As the antisolvent approach depends on the solvent and aqueous phase quality, which includes the concentrations of zein and TEB, variations to the phases will contribute to the NP size and loading efficiency. Increasing the zein: TEB ratio of 5:1 was ideal; higher zein content induced aggregation, whereas lower ratios reduced encapsulation efficiency (Li *et al.* 2019). A solvent:aqueous ratio of 1:5 facilitated rapid nucleation and evaporation of ethanol, leading to smaller particle formation, which will perform better on penetrating the wood matrix. Although a consistent trend was not observed, increasing the aqueous phase volume generally increases solvent diffusion and promotes precipitation, which can lead to smaller particle sizes until a threshold is reached (Martínez Rivas *et al.* 2017). Altogether, the synergistic optimisation of these parameters produced TEB-loaded zein NPs 140.60 ± 4.77 nm with PDI at 0.151 ± 0.043. The loading efficiency of TEB in the zein NP were calculated to be 42.9%.

The levels for each parameter in the study were selected based on preliminary screening tests to establish an operational range that prevents complete nanoparticle aggregation and to provide a simple baseline. Future studies would recommend a multi-factor parameter design to verify the interaction between parameters to improve optimisation.

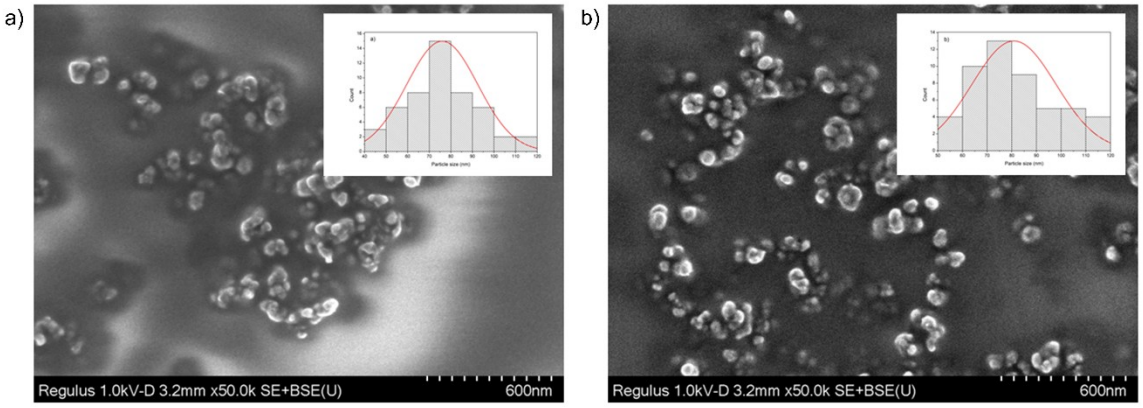
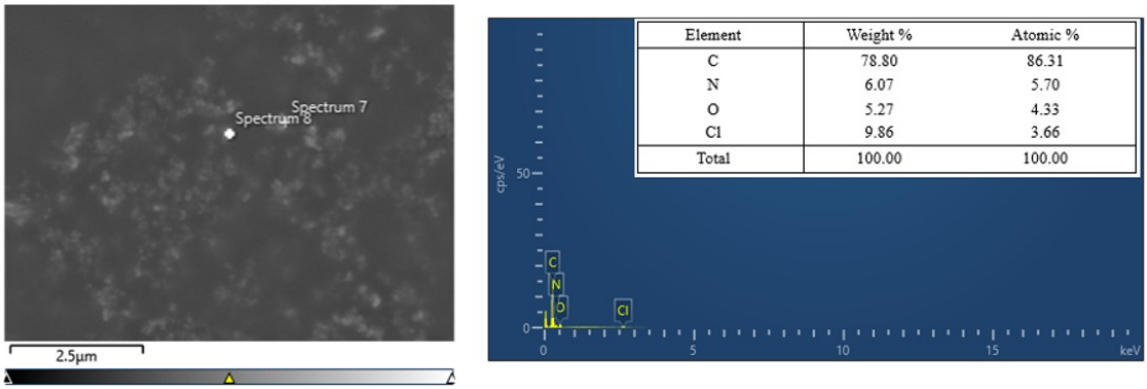


Fig. 1. (a) SEM image of blank zein NPs and its size distribution curve, (b) SEM image of TEB-loaded zein NPs and its size distribution curve

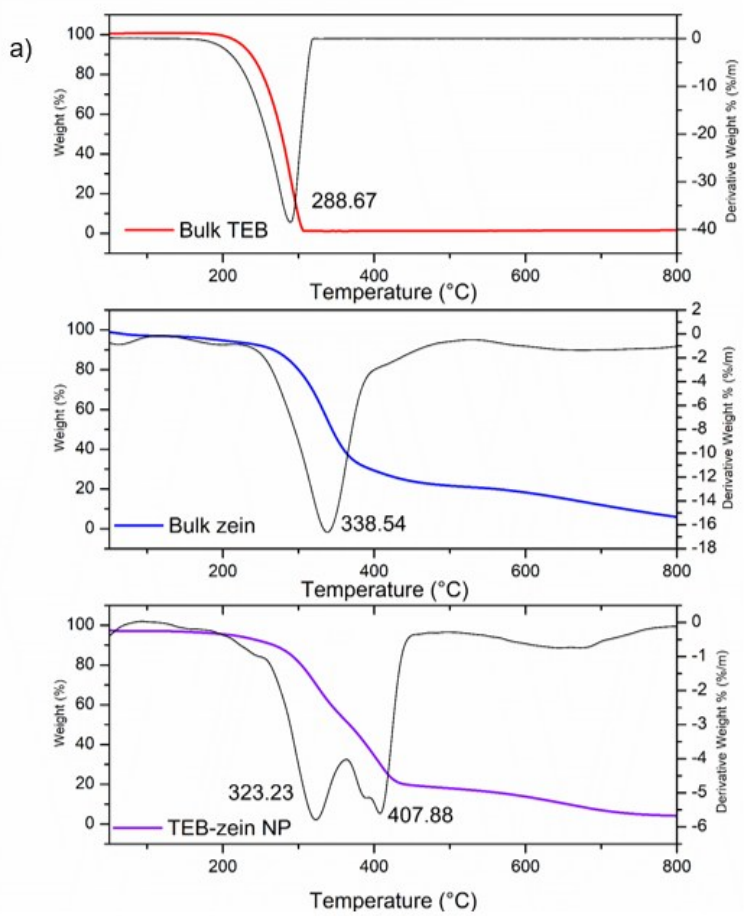
The morphology of the TEB-loaded zein NP were analysed using SEM in Fig. 3a and b. The SEM diagram shows that the shapes of the NPs are generally spherical, with the NPs close to each other. TEB-loaded zein NPs had a slightly larger $z_{average}$ than the blank NPs, recording at 80.88 ± 17.03 nm and 76.01 ± 16.51 nm, respectively. The observed size distribution in the SEM had a low deviation in the $z_{average}$, showing consistency with uniform sizes and low polydispersity in the DLS results. The EDX analysis (Fig. 4) also detected the presence of chlorine in the NPs, which is attributed to TEB. This analysis showed that TEB was successfully incorporated into the zein NPs. UV-Visible

spectroscopy was used to determine the loading efficiency of TEB-loaded zein NP at the wavelength of 220 nm, which coincides with the absorption wavelength range of TEB. The loading efficiencies from the unoptimised and optimised TEB-loaded zein NP were 39.8% and 43.0%, respectively. TEB is incorporated with zein NPs during nanoprecipitation, due to hydrogen bonding between TEB and the zein protein backbone (Liang *et al.* 2015; Želonková *et al.* 2019). The optimised NPs show improvements in loading efficiency but also in hydrodynamic size, which can improve delivery efficiency into the wood matrix.



Element	Weight %	Atomic %
C	78.80	86.31
N	6.07	5.70
O	5.27	4.33
Cl	9.86	3.66
Total	100.00	100.00

Fig. 2. EDX analysis diagram and spot analysis ("Spectrum 8") for TEB-loaded zein NPs



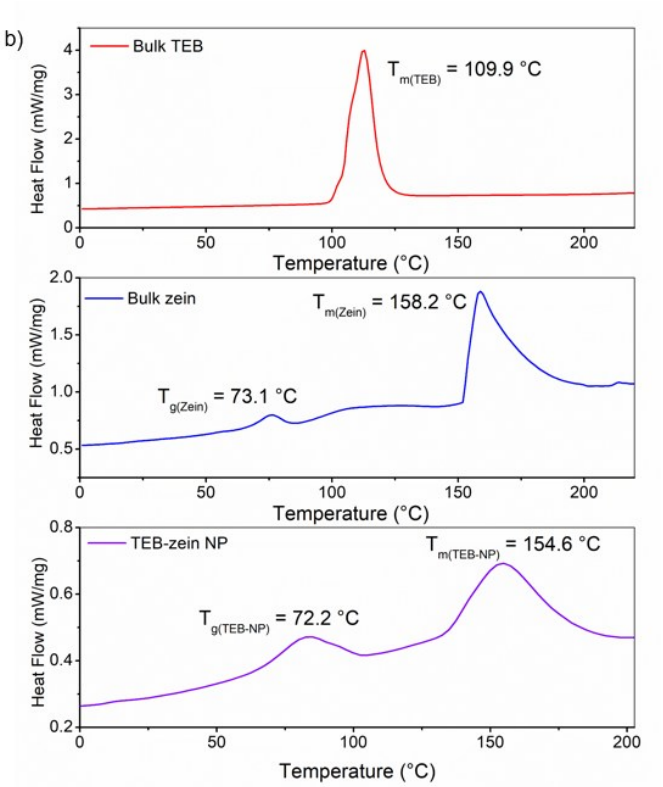


Fig. 3. Thermal analysis of bulk TEB, bulk zein, and TEB-loaded zein NPs: TGA (a) and DSC (b)

The thermal profile for the bulk zein, bulk TEB, and TEB-loaded zein NPs was evaluated with TGA and DSC, as shown in Fig. 5a and b, respectively. From the TGA graph, it is apparent that both bulk zein and bulk TEB had a one-step mass loss, whereas the TEB-loaded zein NPs had a two-step degradation. The distinct peaks in both bulk zein and bulk TEB are attributed to the cleavage of the peptide chains and the triazole ring (Corradini *et al.* 2004; Borucka and Celinski 2019), which results in a one-step degradation. However, the two-step degradation in the TEB-loaded zein NP is likely due to the degradation of TEB incorporated in the NP and followed by the breakdown of the structural formation and physical attraction between TEB and zein (Sun *et al.* 2016). By comparison, TEB-loaded zein NPs retained the thermal stability of bulk zein with similar T_{max}. These findings support the interaction of TEB being incorporated into the zein NP, as there is a slight increase in resistance to thermal degradation. Subsequently, the thermal transitions of bulk zein, bulk TEB and TEB-loaded zein NP were also analysed using DSC to study their thermal characteristics. Zein, being a protein, showed its thermal denaturation around 158.2 °C, but also a small peak at 73.1 °C, which may indicate the evaporation of bound water (Shi *et al.* 2022). Bulk TEB confirms its crystalline structure with the apparent sharp endothermic peak, but this peak was absent in the TEB-loaded zein NP thermograph. This can be explained as TEB losing its crystalline form when incorporated into the zein NP (Wang *et al.* 2022).

Rubberwood Treatment with TEB-loaded Zein NPs

Treatment of rubberwood using TEB-loaded zein NPs was evaluated by determining treatability and chemical retention. The treatability calculated was 284.52 ± 47.70 L/m3, and the chemical retention calculated was 7.11 ± 1.19 kg/m3. Treatability of

rubberwood samples *via* the nanoprecipitation approach was classified as "easy". High treatability was achieved as the NP sizes were within the range of rubber wood vessels, which can range from 82 to 260 µm to facilitate entry for the NPs and allowing deep penetration into the wood structure (Savero *et al.* 2023). The chemical retention calculated also showed good results, indicating that the TEB-loaded zein NPs can be retained in the rubberwood structure and can deliver TEB effectively. Amino acids in zein interact with the wood matrix through hydrogen bonding (Perez *et al.* 2023), enabling affinity of the zein NP to be adsorbed to the structure, ensuring protection.

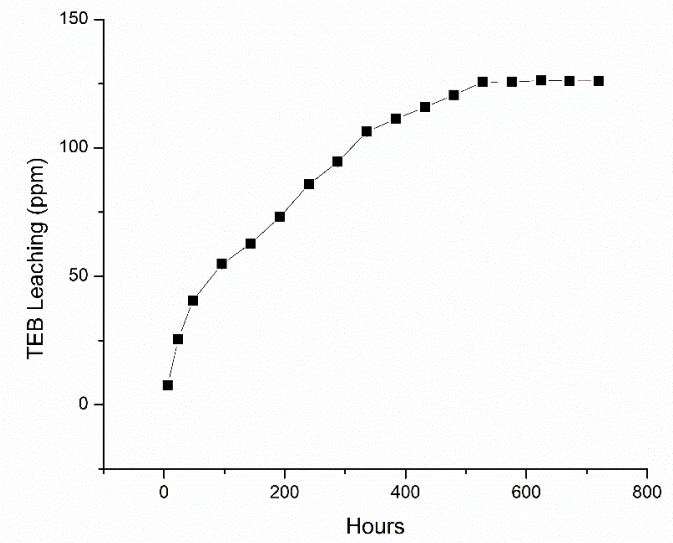


Fig. 4. TEB leaching results of TEB-loaded zein NP treated rubberwood samples for 720 h

From the leaching test results in Fig. 6, consistent gradual leaching of TEB from the zein NP-treated rubberwood samples was observed, reaching a plateau after 528 h with a final leached amount of 126.136 ppm after 720 h. This sustained release is a critical advantage, ensuring continuous preservative availability within the wood matrix for prolonged protection against biodegradation (Liu *et al.* 2001, 2024). The inherent hydrophobicity of zein and its capacity for hydrogen bonding with TEB are instrumental in facilitating this controlled release, a mechanism supported by previous studies (Chuacharoen and Sabliov 2016; Liu *et al.* 2019). The sustained release observed improved retention of the biocide within the wood. This results in enhanced biological efficacy against termites and fungi, improving efficiency and minimizing overall biocide leaching while maintaining protective concentrations.

Biological Efficacy Performance Studies of TEB-loaded Zein NP Treated Wood

The rubberwood samples treated with TEB-loaded zein NPs were tested against brown rot (*Gloeophyllum trabeum*), white rot fungi (*Trametes versicolor*), and subterranean termite (*Coptotermes gestroi*). The effectiveness of the treatment was comparing the untreated control samples with the treated wood samples, where the weight loss percentage was calculated, and the decay rating was assigned based on the weight loss percentage of the wood. The weight loss of the wood samples from the anti-fungal test is listed in Table 2.

Table 2. Weight Loss Percentage and Decay Rating of Control and TEB-loaded Zein NP Treated Wood Samples against Brown Rot and White Rot Fungi

Sample	Brown rot fungi		White rot fungi	
	Weight loss %	Decay rating	Weight loss %	Decay rating
Untreated control	38.48 ± 1.58	Moderately resistant	41.20 ± 0.76	Moderately resistant
TEB-loaded zein NP treated sample	15.68 ± 0.67	Resistant	24.04 ± 0.29	Resistant

Untreated wood samples demonstrated an average weight loss of 41.20 ± 0.76% in the white rot fungi test, while the TEB-loaded zein NP-treated wood samples experienced a weight loss of only 24.04 ± 0.29%. The TEB-loaded zein NP-treated wood samples exhibited a 59.0% reduction in weight loss against brown rot fungi ($t(8) = 2.570$; $p < 0.05$) and a 39.7% reduction against white rot fungi ($t(8) = 2.306$; $p < 0.05$), both showing statistically significant differences at a 95% confidence level compared to the control samples. Additionally, when comparing the results between the two fungal types, a significant difference in weight loss was observed, with the reduction against brown rot fungi being 8.36% greater than that against white rot fungi ($t(8) = -20.58$; $p < 0.05$), indicating marked effectiveness of the TEB-loaded zein NP treatment against brown rot fungi. TEB effectively controls brown rot fungi by disrupting ergosterol biosynthesis in cell membranes; in contrast, white rot fungi are characterized by their production of specialized lignin-modifying enzymes that simultaneously degrade lignin and cellulose (Arantes and Goodell 2014). While recent studies on antifungal approaches such as N-CQD and lignin based coatings operate on positive surface charges and doping (Amini *et al.* 2025; Wang *et al.* 2024b), TEB utilizes producing radicals better than deterring enzyme activity in white rot fungi, hence showing better performance against brown rot fungi.

Table 3. Weight Loss Percentage and Durability Class of Control and TEB-loaded Zein NP Treated Wood Samples against Subterranean Termites

Duration	Samples			
	Control		TEB-loaded zein NP treated sample	
	% Weight loss	Durability	% Weight loss	Durability
Day 7	12.24 ± 1.56	Moderate	4.21 ± 0.24	Highly durable
Day 14	19.54 ± 1.21	Moderate	3.81 ± 0.93	Highly durable
Day 21	23.24 ± 3.27	Moderate	3.33 ± 1.02	Highly durable

The average weight loss percentage of the wood samples from the anti-termite tests is recorded in Table 3. The control wood samples exhibited an average weight loss of 18.3 ± 5.27%, whereas the TEB-loaded zein NP-treated wood samples demonstrated a significantly lower average weight loss of 3.79 ± 0.80%. To assess the statistical significance of the weight loss between the two groups, a Student's t-test was conducted. The TEB-loaded zein NP-treated wood samples ($M = 0.087$, $SD = 0.020$) showed a 79.4% reduction in weight loss, which was statistically significant ($t(18) = 8.457$; $p < 0.05$) compared to the control samples ($M = 0.440$, $SD = 0.124$). This indicates that TEB-loaded zein NP treatment provided substantial protection against subterranean termites. Throughout the 21-day testing period, all treated wood samples were classified as "highly durable," highlighting their effectiveness in termite resistance. Visual assessments in Fig. 7a and b revealed that the untreated control wood samples exhibited significant darkening

and damage from moisture and termite activity, while the TEB-loaded zein NP-treated wood showed minimal damage, with only slight tunnelling observed after 21 days. These findings suggest that the TEB-loaded zein NP treatment offers effective termite protection, significantly reducing both weight loss and physical damage to the wood. As the termite count after the trials did not diminish, the TEB-loaded zein NP acts as a repellent and deters termite feeding instead of killing them, which is similar to extractives or plant essential oils (Verma *et al.* 2009; Little *et al.* 2010).

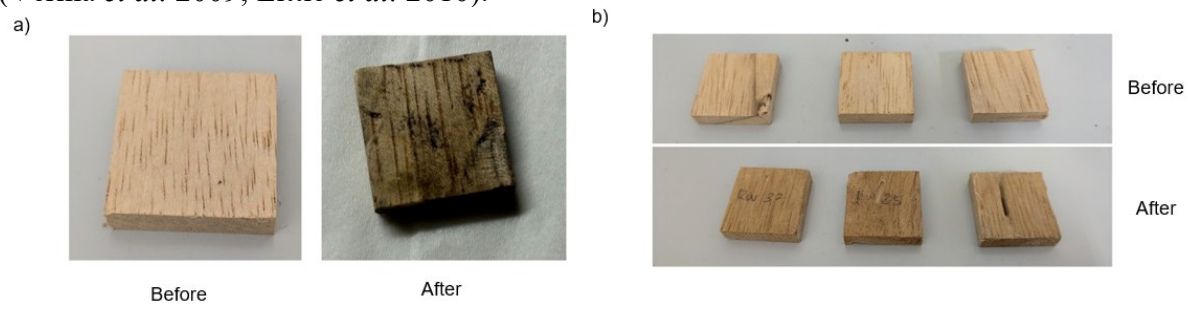


Fig. 5. (a) Untreated control rubberwood sample before and after the anti-termite test, and (b) TEB-loaded zein NP treated rubber wood samples before and after anti-termite test

CONCLUSIONS

1. Tebuconazole (TEB)-loaded zein nanoparticles (NPs) were successfully synthesized and optimized for rubberwood treatment, demonstrating high loading efficiency and superior chemical retention after vacuum pressure impregnation. The TEB-loaded zein NPs provided comprehensive protection of wood against subterranean termites (*Coptotermes gestroi*), brown rot fungi (*Gloeophyllum trabeum*), and white rot fungi (*Trametes versicolor*).
2. Effective wood preservation was achieved at a concentration of 0.025% w/v, which is significantly lower than the 5% w/v concentration specified by the Malaysian Standard (MS360:2006), indicating a major improvement in treatment efficiency.
3. This study demonstrates that tebuconazole-loaded zein NPs can provide a sustainable and effective alternative for wood preservation by enabling the use of significantly lower biocide concentrations while providing sustainable protection to both timber and environment.

ACKNOWLEDGMENTS

This work was supported by the Bridging Grant from Universiti Sains Malaysia [Grant Number R501-LR-RND003-0000000560-0000] and the Royal Society of Chemistry (RSC) Research Fund [Grant Number 304/PKIMIA/6501385/R123]. Z. Ong would like to thank Erasmus Mundus and Postgraduate Research Attachment (PGRA), USM, for supporting his research attachment at the Laboratory of Studies and Research on Wood Material (LERMAB), University of Lorraine, France, and Forest Research Institute Malaysia (FRIM) for providing the wood samples and biological efficacy testing. The authors thank the Platform Green Process for Wood (GP4Wood) of LERMaB (Université de Lorraine- INRAe), F-54000 Nancy, France.

Use of Generative AI

This article utilised OpenAI ChatGPT-4 (May 2026 version) solely for language improvement with rigorous revision to improve the fluency and expression of the article.

REFERENCES CITED

Alade, A. A., Naghizadeh, Z., Wessels, C. B., and Tyhoda, L. (2022). "A review of the effects of wood preservative impregnation on adhesive bonding and joint performance," *Journal of Adhesion Science and Technology*, Taylor & Francis, 36(15), 1593-1617. https://doi.org/10.1080/01694243.2021.1981651

de Albuquerque, N. C. P., Carrão, D. B., Habenschus, M. D., and de Oliveira, A. R. M. (2018). "Metabolism studies of chiral pesticides: A critical review," *Journal of Pharmaceutical and Biomedical Analysis*, Review issue 2017, 147, 89-109. https://doi.org/10.1016/j.jpba.2017.08.011

Amini, S., Erdocia, X., Labidi, J., and Fernández, Á. G. (2025). "Lignin based ecological coatings for improved anti-corrosion resistance," *Progress in Organic Coatings* 200, article 109044. https://doi.org/10.1016/j.porgcoat.2024.109044

Arantes, V., and Goodell, B. (2014). "Current understanding of brown-rot fungal biodegradation mechanisms: A review," in: *Deterioration and Protection of Sustainable Biomaterials*, ACS Symposium Series, American Chemical Society, 3-21. https://doi.org/10.1021/bk-2014-1158.ch001

Araujo, J. T. C. de, Martin-Pastor, M., Pérez, L., Pinazo, A., and Sousa, F. F. O. de. (2021). "Development of anacardic acid-loaded zein nanoparticles: Physical chemical characterization, stability and antimicrobial improvement," *Journal of Molecular Liquids* 332, article 115808. https://doi.org/10.1016/j.molliq.2021.115808

Borucka, M., and Celinski, M. (2019). "Thermal degradation and combustion behavior of antifungal pesticides: triadimenol and tebuconazole," *Chemical Engineering Transactions* 77, 139-144. https://doi.org/10.3303/CET1977024

Čadková, E., Komárek, M., Debord, J., Della Puppa, L., Bordas, F., and Bollinger, J.-C. (2013). "pKa constant determination of two triazole pesticides: Tebuconazole and penconazole," *Journal of Solution Chemistry* 42(5), 1075-1082. https://doi.org/10.1007/s10953-013-0012-z

Campos, L. A. A., Neto, A. F. S., Notonha, M. C. S., de Lima, M. F., Cavalcanti, I. M. F., and Santos-Magalhães, N. S. (2023). "Zein nanoparticles for drug delivery: Preparation methods and biological applications," *International Journal of Pharmaceutics* 635, article 122754. https://doi.org/10.1016/j.ijpharm.2023.122754

Chaud, M., Souto, E. B., Zielinska, A., Severino, P., Batain, F., Oliveira-Junior, J., and Alves, T. (2021). "Nanopesticides in agriculture: Benefits and challenge in agricultural productivity, toxicological risks to human health and environment," *Toxics* 9, article 131. https://doi.org/10.3390/TOXICS9060131

Chen, C., Kuang, Y., Zhu, S., Burgert, I., Keplinger, T., Gong, A., Li, T., Berglund, L., Eichhorn, S. J., and Hu, L. (2020). "Structure–property–function relationships of natural and engineered wood," *Nature Reviews Materials* 5(9), 642-666. https://doi.org/10.1038/s41578-020-0195-z

Chen, J., Saleem, M., Wang, C., Liang, W., and Zhang, Q. (2018). "Individual and combined effects of herbicide tribenuron-methyl and fungicide tebuconazole on soil

earthworm *Eisenia fetida*," *Scientific Reports* 8(1), article 2967. https://doi.org/10.1038/s41598-018-21288-y

Cheremisinoff, N. P., and Rosenfeld, P. E. (2010). "Chapter 1 - Wood-preserving chemicals," in: *Handbook of Pollution Prevention and Cleaner Production*, N. P. Cheremisinoff and P. E. Rosenfeld (eds.), William Andrew Publishing, Oxford, pp. 1-26. https://doi.org/10.1016/B978-0-08-096446-1.10001-2

Chuacharoen, T., and Sabliov, C. M. (2016). "Stability and controlled release of lutein loaded in zein nanoparticles with and without lecithin and pluronic F127 surfactants," *Colloids and Surfaces A: Physicochemical and Engineering Aspects* 503, 11-18. https://doi.org/10.1016/j.colsurfa.2016.04.038

Corradini, E., Mattoso, L. H. C., Guedes, C. G. F., and Rosa, D. S. (2004). "Mechanical, thermal and morphological properties of poly(ε-caprolactone)/zein blends," *Polymers for Advanced Technologies* 15(6), 340-345. https://doi.org/10.1002/pat.478

De Lorenzi, A., Giorgianni, S., and Bini, R. (1999). "High-resolution FTIR spectroscopy of the C—Cl stretching mode of vinyl chloride," *Molecular Physics* 96(1), 101-108. https://doi.org/10.1080/00268979909482942

Díaz-Blancas, V., Medina, D. I., Padilla-Ortega, E., Bortolini-Zavala, R., Olvera-Romero, M., and Luna-Bárcenas, G. (2016). "Nanoemulsion Formulations of fungicide tebuconazole for agricultural applications," *Molecules* 21(10), article 1271. https://doi.org/10.3390/molecules21101271

Emenike, C. U., He, Q., and Koushika, K. (2024). "Pentachlorophenol and its effect on different environmental matrices: The need for an alternative wood preservative," *Sustainable Earth Reviews* 7(1), article 22. https://doi.org/10.1186/s42055-024-00090-x

Hassan, B., Mankowski, M. E., and Kirker, G. T. (2021). "Evaluation of heartwood extracts combined with linseed oil as wood preservatives in field tests in southern Mississippi, USA," *Insects* 12(9), 803-803. https://doi.org/10.3390/INSECTS12090803/S1

Hu, K., and McClements, D. J. (2014). "Fabrication of surfactant-stabilized zein nanoparticles: A pH modulated antisolvent precipitation method," *Food Research International* 64, 329-335. https://doi.org/10.1016/J.FOODRES.2014.07.004

Hu, K., and McClements, D. J. (2015). "Fabrication of biopolymer nanoparticles by antisolvent precipitation and electrostatic deposition: Zein-alginate core/shell nanoparticles," *Food Hydrocolloids* 44, 101-108. https://doi.org/10.1016/j.foodhyd.2014.09.015

Hu, Z., Ballinger, S., Pelton, R., and Cranston, E. D. (2015). "Surfactant-enhanced cellulose nanocrystal Pickering emulsions," *Journal of Colloid and Interface Science* 439, 139-148. https://doi.org/10.1016/J.JCIS.2014.10.034

Islam, M. N., Ando, K., Yamauchi, H., Kamikawa, D., Harada, T., Khalil, H. P. S. A., and Hattori, N. (2014). "Impregnation of laser incised wood of Douglas fir and Japanese cedar by dipping (passive impregnation) in solutions of copper azole (CuAz-B) and a fire retardant (PPC)," *Holzforschung* 68(3), 353-360. https://doi.org/10.1515/hf-2013-0140

Jakob, M., Mahendran, A. R., Gindl-Altmutter, W., Bliem, P., Konnerth, J., Müller, U., and Veigel, S. (2022). "The strength and stiffness of oriented wood and cellulose-fibre materials: A review," *Progress in Materials Science* 125, article 100916. https://doi.org/10.1016/j.pmatsci.2021.100916

Kato, T., Hatakeyama, T., and Sugawara, K. (2021). "Release behavior of arsenic, chromium, and copper during heat treatments of CCA-treated wood," *Journal of Material Cycles and Waste Management* 23(4), 1636-1645. https://doi.org/10.1007/S10163-021-01246-Z/METRICS

Khademibami, L., and Bobadilha, G. S. (2022). "Recent developments studies on wood protection research in academia: A review," *Frontiers in Forests and Global Change* 5, 793177-793177. https://doi.org/10.3389/FFGC.2022.793177/BIBTEX

Lebow, S. T. (2010). Chapter 15: *Wood Preservation*, United States Department of Agriculture Forest Service.

Li, H., Wang, D., Liu, C., Zhu, J., Fan, M., Sun, X., Wang, T., Xu, Y., and Cao, Y. (2019). "Fabrication of stable zein nanoparticles coated with soluble soybean polysaccharide for encapsulation of quercetin," *Food Hydrocolloids* 87, 342-351. https://doi.org/10.1016/j.foodhyd.2018.08.002

Liang, H., Zhou, B., Li, J., Xu, W., Liu, S., Li, Y., Chen, Y., and Li, B. (2015). "Supramolecular design of coordination bonding architecture on zein nanoparticles for pH-responsive anticancer drug delivery," *Colloids and Surfaces B: Biointerfaces*, 136, 1224-1233. https://doi.org/10.1016/j.colsurfb.2015.09.037

Little, N. S., Schultz, T. P., and Nicholas, D. D. (2010). "Termite-resistant heartwood. Effect of antioxidants on termite feeding deterrence and mortality," *Holzforschung* 64(3), 395-398. https://doi.org/10.1515/hf.2010.053

Liu, J., Yu, H., Kong, J., Ge, X., Sun, Y., Mao, M., Wang, D. Y., and Wang, Y. (2024). "Preparation, characterization, stability, and controlled release of chitosan-coated zein/shellac nanoparticles for the delivery of quercetin," *Food Chemistry* 444, article 138634. https://doi.org/10.1016/j.foodchem.2024.138634

Liu, Q., Jing, Y., Han, C., Zhang, H., and Tian, Y. (2019). "Encapsulation of curcumin in zein/ caseinate/sodium alginate nanoparticles with improved physicochemical and controlled release properties," *Food Hydrocolloids* 93, 432-442. https://doi.org/10.1016/j.foodhyd.2019.02.003

Liu, Y., Yan, L., Heiden, P., and Laks, P. (2001). "Use of nanoparticles for controlled release of biocides in solid wood," *Journal of Applied Polymer Science* 79(3), 458-465. https://doi.org/10.1002/1097-4628(20010118)79:3<458::AID-APP80>3.0.CO;2-H

Martínez Rivas, C. J., Tarhini, M., Badri, W., Miladi, K., Greige-Gerges, H., Nazari, Q. A., Galindo Rodríguez, S. A., Román, R. Á., Fessi, H., and Elaissari, A. (2017). "Nanoprecipitation process: From encapsulation to drug delivery," *International Journal of Pharmaceutics* 532(1), 66-81. https://doi.org/10.1016/J.IJPHARM.2017.08.064

Nazarpour, F., Abdullah, D. K., Abdullah, N., and Zamiri, R. (2013). "Evaluation of biological pretreatment of rubberwood with white rot fungi for enzymatic hydrolysis," *Materials* 6(5), 2059-2073. https://doi.org/10.3390/ma6052059

Ohgami, N., Yamanoshita, O., Thang, N. D., Yajima, I., Nakano, C., Wenting, W., Ohnuma, S., and Kato, M. (2015). "Carcinogenic risk of chromium, copper and arsenic in CCA-treated wood," *Environmental Pollution* 206, 456-460. https://doi.org/10.1016/j.envpol.2015.07.041

Ong, Z., Tan, S. L., Arip, M. N. M., Lipeh, S., and Lee, H. L. (2023). "Optimising incorporation of tebuconazole via chitosan polymeric nanoparticles for semantan bamboo preservation," *Malaysian Journal of Chemistry* 25(2), 32-42. https://doi.org/10.55373/MJCHEM.V25I2.32

Patel, A. R., Bouwens, E. C. M., and Velikov, K. P. (2010). "Sodium caseinate stabilized zein colloidal particles," *Journal of Agricultural and Food Chemistry* 58(23), 12497-12503. https://doi.org/10.1021/JF102959B/SUPPL_FILE/JF102959B_SI_003.PDF

Perez, L., Hafidi, Z., Pinazo, A., García, M. T., Martín-Pastor, M., and Sousa, F. F. O. de. (2023). "Zein nanoparticles containing arginine-phenylalanine-based surfactants: stability, antimicrobial and hemolytic activity," *Nanomaterials* 13(1), article 200. https://doi.org/10.3390/nano13010200

Podaralla, S., and Perumal, O. (2010). "Preparation of zein nanoparticles by pH controlled nanoprecipitation," *Journal of Biomedical Nanotechnology* 6(4), 312-317. https://doi.org/10.1166/jbn.2010.1137

Ramage, M. H., Burridge, H., Busse-Wicher, M., Fereday, G., Reynolds, T., Shah, D. U., Wu, G., Yu, L., Fleming, P., Densley-Tingley, D., Allwood, J., Dupree, P., Linden, P. F., and Scherman, O. (2017). "The wood from the trees: The use of timber in construction," *Renewable and Sustainable Energy Reviews* 68, 333-359. https://doi.org/10.1016/j.rser.2016.09.107

da Rosa, C. G., de Oliveira Brisola Maciel, M. V., de Carvalho, S. M., de Melo, A. P. Z., Jummes, B., da Silva, T., Martelli, S. M., Villetti, M. A., Bertoldi, F. C., and Barreto, P. L. M. (2015). "Characterization and evaluation of physicochemical and antimicrobial properties of zein nanoparticles loaded with phenolics monoterpenes," *Colloids and Surfaces A: Physicochemical and Engineering Aspects* 481, 337-344. https://doi.org/10.1016/j.colsurfa.2015.05.019

Saad, W. S., and Prud'homme, R. K. (2016). "Principles of nanoparticle formation by flash nanoprecipitation," *Nano Today* 11(2), 212-227. https://doi.org/10.1016/j.nantod.2016.04.006

Savero, A. M., Kim, J. H., Purusatama, B. D., Prasetia, D., Park, S. H., Van Duong, D., and Kim, N. H. (2023). "Characterization of anatomical and non-anatomical properties for the identification of six commercial wood species from Vietnamese plantation forests," *Forests* 14(3), article 496. https://doi.org/10.3390/f14030496

Shi, W., Li, S., Wang, X., Li, S., Zhang, X., and Hou, F. (2022). "An electrostatic self-assembly approach to prepare tebuconazole nanoparticles with improved sustained release and enhanced antifungal activity," *Colloids and Surfaces B: Biointerfaces* 216, article 112587. https://doi.org/10.1016/j.colsurfb.2022.112587

Shigematsu, A., Mizoue, N., Kajisa, T., and Yoshida, S. (2011). "Importance of rubberwood in wood export of Malaysia and Thailand," *New Forests* 41(2), 179-189. https://doi.org/10.1007/s11056-010-9219-7

Sivasankar, K., Pathak, A., and Jain, K. (2024). "Effect of Tween 80 and Pluronic 127 on the stabilization of zein nanocarriers for the delivery of piperine," *Food Research International* 197, article 115202. https://doi.org/10.1016/j.foodres.2024.115202

Sun, C., Dai, L., He, X., Liu, F., Yuan, F., and Gao, Y. (2016). "Effect of heat treatment on physical, structural, thermal and morphological characteristics of zein in ethanol-water solution," *Food Hydrocolloids* 58, 11-19. https://doi.org/10.1016/j.foodhyd.2016.02.014

Tarmian, A., Zahedi Tajrishi, I., Oladi, R., and Efhamisisi, D. (2020). "Treatability of wood for pressure treatment processes: A literature review," *European Journal of*

Wood and Wood Products 78(4), 635-660. https://doi.org/10.1007/S00107-020-01541-W

Teng, T. J., Arip, M. N. M., Ng, E. P., and Lee, H. L. (2021). "Incorporation of chlorothalonil into polylactic acid-co-polyethylene glycol nanoparticles for rubberwood preservation," *European Journal of Wood and Wood Products* 79(2), 499-508. https://doi.org/10.1007/S00107-020-01630-W

Teoh, Y. P., Mat Don, M., and Ujang, S. (2011). "Assessment of the properties, utilization, and preservation of rubberwood (*Hevea brasiliensis*): A case study in Malaysia," *Journal of Wood Science* 57, 255-266. https://doi.org/10.1007/s10086-011-1173-2

Thaler, N., and Humar, M. (2014). "Copper leaching from copper-ethanolamine treated wood: comparison of field test studies and laboratory standard procedures," *BioResources* 9(2), 3038-3051. https://doi.org/10.15376/biores.9.2.3038-3051

Tleuova, A. B., Wielogorska, E., Talluri, V. S. S. L. P., Štěpánek, F., Elliott, C. T., and Grigoriev, D. O. (2020). "Recent advances and remaining barriers to producing novel formulations of fungicides for safe and sustainable agriculture," *Journal of Controlled Release* 326, 468-481. https://doi.org/10.1016/j.jconrel.2020.07.035

Townsend, T., Tolaymat, T., Solo-Gabriele, H., Dubey, B., Stook, K., and Wadanambi, L. (2004). "Leaching of CCA-treated wood: Implications for waste disposal," *Journal of Hazardous Materials* 114(1–3), 75-91. https://doi.org/10.1016/j.jhazmat.2004.06.025

Vani, C. N., Prajwal, S., Sundararaj, R., and Dhamodaran, T. K. (2022). "Chemical Preservatives in wood protection," *Science of Wood Degradation and its Protection* 2022, 559-587. https://doi.org/10.1007/978-981-16-8797-6_16

Verma, M., Sharma, S., and Prasad, R. (2009). "Biological alternatives for termite control: A review," *International Biodeterioration & Biodegradation* 63(8), 959-972. https://doi.org/10.1016/j.ibiod.2009.05.009

Wang, L., Wang, P., Li, Y., Liu, S., Wu, L., Zhang, W., and Chen, C. (2024a). "A novel strategy to enhance the pH stability of zein particles through octenyl succinic anhydride-modified starch: The role of preparation pH," *Foods* 13(2), article 303. https://doi.org/10.3390/foods13020303

Wang, L., Wang, T., Hao, R., and Wang, Y. (2024b). "Construction strategy and mechanism of a novel wood preservative with excellent antifungal effects," *Molecules* 29(5), article 1013. https://doi.org/10.3390/molecules29051013

Wang, Q., Tang, Y., Yang, Y., Lei, L., Lei, X., Zhao, J., Zhang, Y., Li, L., Wang, Q., and Ming, J. (2022). "The interaction mechanisms, and structural changes of the interaction between zein and ferulic acid under different pH conditions," *Food Hydrocolloids* 124, article 107251. https://doi.org/10.1016/j.foodhyd.2021.107251

Wong, T. H., Saifizul, A., Ramli, R., and Soong, M. F. (2023). "The timbre of sape: Identifying the sound quality in music instrument making," *Journal of New Music Research* 52(1), 3-18. https://doi.org/10.1080/09298215.2023.2290272

Xing, M., Zhao, H., Ahmed, R., Wang, X., Liu, J., Wang, J., Guo, A., and Wang, M. (2022). "Fabrication of resveratrol-loaded zein nanoparticles based on flash nanoprecipitation," *Colloids and Surfaces A: Physicochemical and Engineering Aspects* 654, article 129829. https://doi.org/10.1016/j.colsurfa.2022.129829

Želonková, K., Havadej, S., Verebová, V., Holečková, B., Uličný, J., and Staničová, J. (2019). "Fungicide tebuconazole influences the structure of human serum albumin

molecule," *Molecules* 24(17), article 3190. https://doi.org/10.3390/molecules24173190

Zou, T., Li, Z., Percival, S. S., Bonard, S., and Gu, L. (2012). "Fabrication, characterization, and cytotoxicity evaluation of cranberry procyanidins-zein nanoparticles," *Food Hydrocolloids* 27(2), 293-300. https://doi.org/10.1016/j.foodhyd.2011.10.002

Article submitted: January 28, 2026; Peer review completed: April 4, 2026; Revised version received: May 31, 2026; Accepted: June 17, 2026; Published: July 7, 2026.
DOI: 10.15376/biores.21.3.7801-7822

APPENDIX

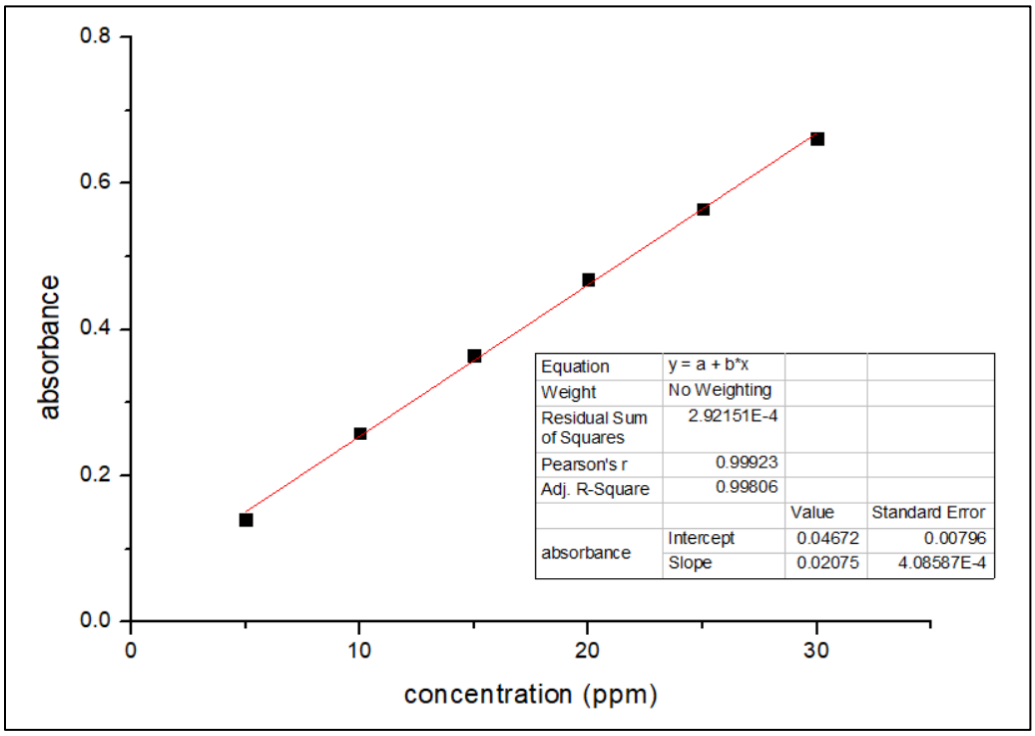


Fig. A1. Mean calibration curve of tebuconazole in 85% ethanol at wavelength of 221 nm

Table A1. Statistical Analysis for Accuracy of the Method using Tebuconazole (n = 5)

Concentration of tebuconazole, ppm	Measured average% recovery	% RSD
80%	101.52	0.27
100%	102.31	0.75
120%	100.26	0.34

Table A2. Statistical Analysis for Precision (Intraday and Interday) of the Method using Tebuconazole (n = 5)

Concentration of tebuconazole, ppm	Intraday		Interday	
	Measured concentration, ppm (Mean ± SD)	% RSD	Measured concentration, ppm (Mean ± SD)	% RSD
5	5.92 ± 0.57	8.59	5.12 ± 0.38	6.55
10	9.94 ± 0.52	4.76	9.54 ± 0.72	7.05
15	14.90 ± 0.54	3.30	15.84 ± 0.78	4.73
20	20.97 ± 0.88	3.86	22.45 ± 1.00	4.33
25	26.70 ± 0.71	2.64	28.43 ± 1.03	3.56
30	31.90 ± 0.79	2.38	34.17 ± 1.72	4.94

Table A3. Statistical Analysis for Reproducibility of the Method using Tebuconazole (n = 5)

Concentration of tebuconazole, ppm	Measured concentration, ppm (Mean ± SD) at UV-Vis 1	% RSD	Measured concentration, ppm (Mean ± SD) at UV-Vis 2	% RSD
30	32.49 ± 0.29	0.88	32.44 ± 0.14	0.44

Table A4. Permeability Classification *(Teng et al. 2021)*

Permeability class	Absorption of preservative in 1 m^{-3} of timber
Very easy	Over 320
Easy	240 – 320
Average	160 – 240
Moderate difficult	80 – 160
Difficult	< 80

Table A5. Wood Resistance Rating for Termite Test (Teng *et al.* 2021)

Rating Class	Description
Highly durable	< 5% weight loss
Durable	5.1 – 10% weight loss
Moderately durable	10.1 – 30% weight loss
Slightly durable	30.1 – 50% weight loss
Non-durable	>50% weight loss

Table A6. Weight loss classification of wood samples for anti-fungi test (Teng *et al.* 2021)

Decay rating	Mean% weight loss
Highly resistant	0 – 10
Resistant	11 – 24
Moderately resistant	25 – 44
Slightly resistant	>45

Table A7. Effect of Zein Concentration on TEB-loaded Zein Nanoparticles, with Tween 80 Concentration, Dropping Rate, and pH (n = 3)

Sample	Zein concentration (%w/v)	$Z_{average}$ (nm)	Polydispersity index, PDI
N1	0.010	582.33 ± 99.95	0.791
N2	0.015	365.67 ± 82.71	0.683
N3	0.020	319.77 ± 27.85	0.562
N4	0.025	195.17 ± 16.61	0.394
N5	0.030	233.23 ± 33.31	0.510

Table A8. Effect of Tween 80 Concentration on TEB-loaded Zein Nanoparticles, with Zein Concentration, Dropping Rate, and pH (n = 3)

Sample	Tween 80 concentration (%w/v)	$Z_{average}$ (nm)	Polydispersity index, PDI
N6	0.015	255.37 ± 13.23	0.447
N7	0.020	223.80 ± 8.06	0.525
N8	0.025	199.03 ± 15.73	0.465
N9	0.030	197.67 ± 20.41	0.444
N10	0.035	146.40 ± 10.66	0.446

Table A9. Effect of Dropping Rate on TEB-loaded Zein Nanoparticles, with Zein Concentration, Tween 80 Concentration, and pH (n = 3)

Sample	Dropping rate, mL/min	$Z_{average}$ (nm)	Polydispersity index, PDI
N11	0.2	228.27 ± 20.50	0.468
N12	0.4	249.20 ± 34.14	0.645
N13	0.6	122.30 ± 1.22	0.304
N14	0.8	176.17 ± 4.10	0.298
N15	1.0	420.60 ± 223.27	0.793

Table A10. Effect of pH on TEB-loaded Zein Nanoparticles, with Fixed Zein Concentration, Tween 80 Concentration, and Dropping Rate (n = 3)

Sample	pH (±0.2)	$Z_{average}$ (nm)	Polydispersity index, PDI
N16	3	159.22 ± 9.07	0.251
N17	4	140.60 ± 4.77	0.151
N18	5	2913.60 ± 754.41	0.435
N19	6	345.06 ± 99.11	0.484
N20	7	250.50 ± 12.15	0.164
N21	8	308.84 ± 13.48	0.248

Table A11. Effect of Zein: TEB Ratio on TEB-loaded Zein Nanoparticles, with Fixed Zein Concentration, Tween 80 Concentration, Dropping Rate, and pH (n = 3)

Sample	Zein: TEB ratio	$Z_{average}$ (nm)	Polydispersity index, PDI
N22	2:1	278.78 ± 55.64	0.338
N23	4:1	230.20 ± 21.76	0.526
N24	5:1	208.34 ± 8.24	0.391
N25	8:1	214.76 ± 11.50	0.558

Table A12. Effect of Solvent: Aqueous Ratio on TEB-loaded Zein Nanoparticles, with Fixed Zein Concentration, Tween 80 Concentration, Dropping Rate, pH, and Zein: TEB Ratio (n = 3)

Sample	Solvent: aqueous ratio	$Z_{average}$ (nm)	Polydispersity index, PDI
N26	1:2.5	125.96 ± 21.24	0.327
N27	1:5	81.94 ± 9.66	0.312
N28	1:10	125.34 ± 37.69	0.340